

Particle Flux, Crossphase, and Turbulent Amplitude Suppression Scaling with Bias-driven Variation of Flow Shear on the Large Plasma Device

D.A. Schaffner,¹ T.A. Carter,¹ G.D. Rossi,¹ D.S. Guice,¹ J.E. Maggs,¹ S. Vincena,¹ and B. Friedman¹
Department of Physics and Astronomy, University of California, Los Angeles

(Dated: 16 November 2012)

Continuous control over azimuthal flow and shear in the edge of the Large Plasma Device (LAPD) has been achieved using a biasable limiter which has allowed a careful study of the effect of flow shear on pressure-gradient-driven turbulence and transport in LAPD. The combination of such fine shear variation in a fully turbulent plasma along with the detailed spatial diagnostic capabilities on LAPD makes the experiment a useful testbed for verification and comparison to various shear suppression models. Power-law fits are made to the density and radial velocity fluctuation amplitude, particle flux, relative crossphase between density and velocity fluctuations and radial correlation length as functions of both weak and strong shearing.

I. INTRODUCTION

Suppression of turbulence and transport by increased flow shear has been observed on a multitude of different plasma experiments in both spontaneous flow states as well as bias driven flow. While the necessity of cross-field flow shear has been generally accepted for the successful high confinement operation of current and future plasma devices, the exact physical mechanisms connecting increased flow shear to the suppression of turbulence and transport is not fully understood. Having a quantitative grasp as to how turbulence and confinement levels scale with flow shear as well as the ability to make predictions as to what mechanisms will dominate in various scenarios is vital for extrapolation to larger future machines such as ITER. The primary goal of this paper is to provide a detailed experimental dataset for comparison and verification of various models which make predictions as to the relative magnitude of suppression for various turbulent quantities. A further goal is to provide insight into the physical mechanisms actually at work in such suppression observations.

Control of poloidal or azimuthal flow shear in a turbulent plasma has been previously achieved in a number of toroidal devices using biased electrodes in order to create cross-field flow through the generation of cross-field current. In particular, biasing experiments conducted on TEXTOR have yielded results that have been compared to shear suppression models for both density fluctuation amplitude and particle flux showing promising comparisons. Using a recent dataset on LAPD where a detailed scan of sheared flow in a turbulent, linear field line plasma was made using a biased limiter, we hope to extend such shear suppression model verification studies. The recent data set demonstrated the suppression and modification of a number of turbulent quantities with increase shearing rate including cross-field particle flux, density and radial ExB velocity fluctuations, the relative crossphase between said fluctuations, and radial correlation length. Moreover, the scan included data points in both the weak and strong shearing regime, as defined by the ratio of shearing rate to inverse autocorrelation time providing the ability for comparison to models which make sepa-

rate predictions for each regime.

II. SUPPRESSION MODELING

Shear suppression models based on the spatial decorrelation of turbulent structures has been the most common approach to describing both the physical mechanism underlying suppression as well as for making scaling predictions. The basic premise underlying these models is the effect of shearing to break apart or shrink turbulent eddies and consequently decrease both fluctuation amplitude and transport step size. Variation in the model predictions arise from differences in shearing regime, source of turbulent drive (i.e. Ion Temperature Gradient, Interchange Drive or Pressure-Gradient Drive), as well as consideration of passive versus dynamic scalars. Recently, other approaches to explaining shear suppression have been made including the enhancement of coupling to damped eigenmodes by sheared flow (Terry) and by nonlinear shifts in the wavenumber spectrum of the turbulence by shearing. However, this paper will focus on the varying decorrelation models which include scaling predictions.

Two of the earliest of decorrelation models were developed by Biglari, Diamond, Terry in 1990 and Shaing in 1990. The BDT theory attempts a generalized analysis of the transport of any passive scalar in a mean sheared flow in the strong-shear regime with constant drive gradient. BDT the prediction that normalized fluctuation amplitude scales directly with shear to the -2/3 power as in,

$$\frac{\langle |\tilde{\xi}|^2 \rangle}{\langle |\tilde{\xi}|^2 \rangle_{\gamma_s=0}} \sim (\gamma_s \tau_{ac})^{-2/3} \quad (1)$$

where η can be any quantity such as density or temperature. Conversely, the Shaing model predicts a scaling of the form,

$$\frac{\langle |\tilde{\xi}|^2 \rangle}{\langle |\tilde{\xi}|^2 \rangle_{\gamma_s=0}} \sim 1 - \alpha (\gamma_s \tau_{ac})^2 \quad (2)$$

for fluctuation amplitude for the weak shear regime, where α is a constant containing mode number information. An attempt to incorporate the BDT and Shaing models was made by Zhang and Mahajan by expanding the model to incorporate the self-consistent modification of the diffusion and spectrum through fluctuation changes by the flow shear (allowing for a distinction between weak and strong turbulence regimes in the shearing model). The resulting model shows correspondence to the Shaing model in the weak shearing regime while the BDT model is recovered in the strong shearing regime but only for the case where diffusion is unchanged by fluctuation amplitude changes. Furthermore, they extend the model to incorporate the effect of changes in gradient length, showing that shear suppression of fluctuation amplitude is enhanced by a steeper equilibrium gradient.

Work by Terry and Ware in 1996, 1997 made predictions for the effect of shearing on particle transport specifically in a resistive pressure-gradient driven turbulence state. Their work predicted a decrease in flux as a $\Gamma_p \sim 1 - \gamma_s^2$ model in the weak shear limit as well as predicting a decrease in the cosine of the crossphase between density and radial velocity fluctuations also of the form $1 - \omega_s^2$. They, too, incorporated the modification of the pressure gradient formulating an expression for shearing suppression of radial particle diffusivity of the form,

$$\frac{D}{D_{\gamma_s=0}} \sim 1 - \beta(\gamma_s)^2 \quad (3)$$

where β is a constant containing the linear growth rate and radial mode width.

Further work by Terry, Newman and Ware examined the modification of flux in the strong shearing regime for a non-mode-specific turbulence system, predicting a direct scaling of $\Gamma_p \sim \gamma_s^{-4}$ overall, with fluctuation amplitude reductions contributing one power while crossphase reduction contributed three powers, suggesting both a strong dependence of flux on shear as well as an implication that the crossphase can be the dominant flux suppression mechanism rather than the fluctuation amplitude. However, Kim and Diamond in 2003 recast the decorrelation model to include resonance absorption between the shear flow and fluctuations overall suggesting a much weaker dependence of flux on shear, $\Gamma_p \sim \gamma_s^{-1}$, and even weaker dependence of crossphase, $\cos(\theta_{nv_r}) \sim \gamma_s^{-1/6}$, while fluctuations decreased as $|\tilde{n}|^2 \sim \gamma_s^{-5/3}$. Additional work in 2004 added the effect of treating the fluctuating flows dynamically in an interchange driven turbulent plasma which allowed for a prediction for the decrease in fluctuating radial velocity as a function of shear scaling as $|\tilde{v}_r|^2 \sim \gamma_s^{-3}$ in weak shear, and $|\tilde{v}_r|^2 \sim \gamma_s^{-4}$ in strong shearing.

Most recently, a 2006 paper by Leconte found different scalings for flux, fluctuations and crossphase in the strong shear regime depending on relative shearing strength relative to a characteristic time and shearing spatial gradient relative to the inhomogeneity gradient. Work by

Newton and Kim in 2011 has utilized numerical simulations to determine shearing scalings in a generic model.

III. BIAS SHEARING EXPERIMENTS ON LAPD

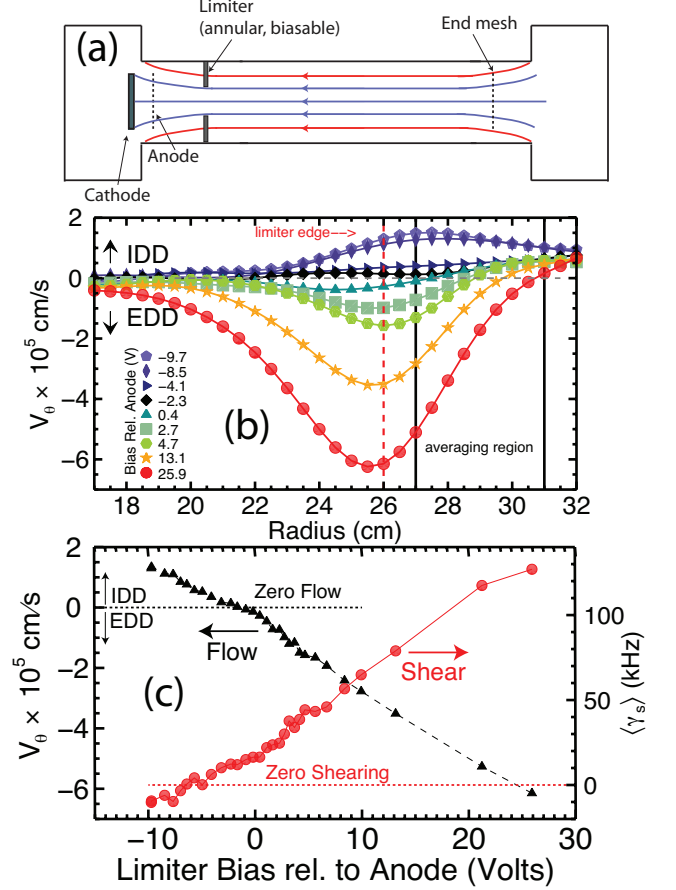


FIG. 1. (a) Diagram of the LAPD device showing annular limiter. (b) Velocity profiles using plasma potential from swept measurements. (c) Flow at the limiter edge (black, triangles) and mean shearing rate, averaged over $27 < r < 31$ cm (red, circles).

The Large Plasma Device¹⁹ (LAPD) is a 17m long, ~ 60 cm diameter cylindrical plasma produced by a barium-oxide coated nickel cathode. In the experiments reported here, a plasma of density $\sim 2 \times 10^{12}$ cm $^{-3}$ and peak temperature of 8eV is produced in a uniform solenoidal magnetic field of 1000G. Measurements of electron density, electron temperature, and potential (both plasma potential and floating potential) are made using Langmuir probes. Measurements of ion saturation current ($I_{\text{sat}} \propto n_e \sqrt{T_e}$) and floating potential (V_f) are taken with a 9-tip Langmuir probe (flush-mount tantalum tips) while temperature and plasma potential are determined using a swept Langmuir probe. I_{sat} fluctuations are taken as a proxy for density fluctuations for the measurements reported in this work. Density profiles are determined

by scaling averaged I_{sat} profiles to line-averaged interferometer measurements of density. Turbulent particle flux $\Gamma \propto \langle \tilde{n}_e \tilde{E}_\theta \rangle$ is determined through correlating density fluctuations from one tip of this probe with azimuthal electric field fluctuations (E_θ) derived from floating potential fluctuations on two azimuthally separated tips. Azimuthal $E \times B$ flow is computed using the swept-probe-derived plasma potential.

A large annular aluminum limiter was installed in LAPD to provide a parallel boundary condition for the edge plasma and is biased relative to the cathode of the plasma source to control plasma potential and cross-field flow. The limiter is an iris-like design with four radially movable plates located 2.5m from the cathode as shown schematically in Fig. 1(a). The limiters create a 52cm diameter aperture; downstream of the limiter, plasma on field lines with radial location $r > 26\text{cm}$ has the limiter as a conducting end parallel boundary condition and plasma on field lines for $r < 26\text{cm}$ has the anode/cathode of the source region as a parallel boundary condition. An electrically floating conducting end mesh terminates the plasma on the far end of the device. A capacitor bank and transistor switch supply a voltage pulse to the limiter. The bias pulse lasts 5ms during the flat-top of the $\sim 15\text{ms}$ plasmadischarge. The limiter is biased from $\sim 10\text{V}$ below to 50V above the anode potential. Typically, plasma potential in the core LAPD plasma (plasma on field lines that connect to the source region) is very close to the anode voltage and the cathode sits near ground (vacuum chamber wall). The anode potential is above the cathode potential by the discharge voltage, which was $\sim 40\text{V}$ during these experiments.

A recent experiment on the LAPD¹ demonstrated the ability to achieve fine and continuous control of steady-state azimuthal flow and flow shear through the use of biasable limiters. The spontaneous flow in the ion diamagnetic drift direction was first nullified and then reversed into the electron diamagnetic drift direction as bias was increased. This resulted in a continuous scan of flow shear states up to a shearing rate, γ_s , of about five times the turbulent inverse autocorrelation time τ_{ac}^{-1} as measured in the unsheared state. Measurements of radial particle flux, density profiles and fluctuation amplitude showed suppression of all three quantities as a function of normalized sheared flow. Figure ??? shows the experimental results for measurements of density fluctuation amplitude, ExB or radial velocity amplitude, crossphase, particle flux, radial correlation length, and diffusivity as a function of normalized shearing rate. The shearing rates achieved span two regimes: a weak-shear regime where $\gamma_s \tau_{ac} < 1$ and a strong-shear regime where $\gamma_s \tau_{ac} > 1$.

IV. EXPERIMENTAL SCALING

The various experimentally measured quantities as functions of normalized shearing rate were fit to a power

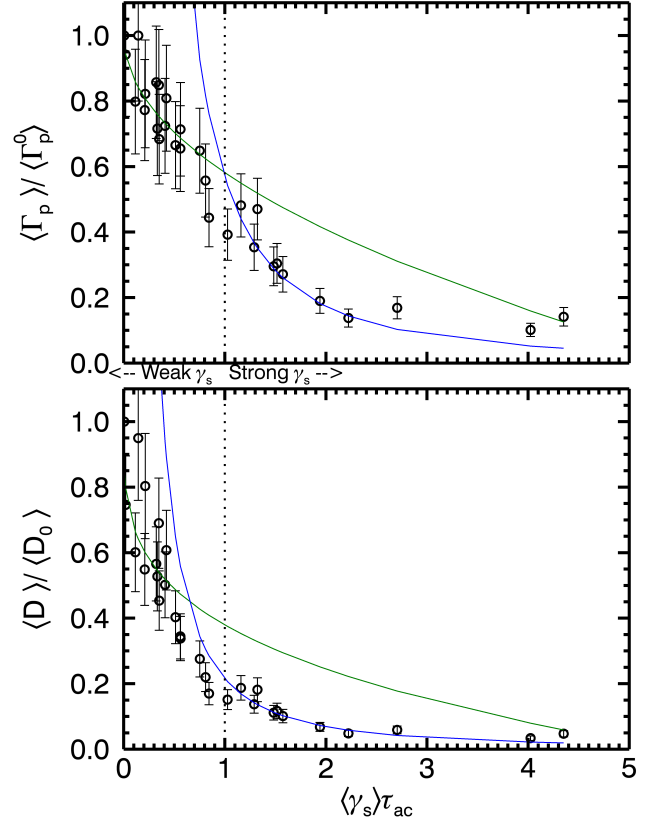


FIG. 2. Scaling of (a) radial particle flux and (b) diffusion coefficient each normalized to the value at minimum shear, $\Gamma_p^0 = 1.7 \times 10^{16} \text{cm}^{-2}$ and $D_0 = 36.7 \text{m}^2/\text{s}$. The green curves correspond to $1 - \gamma_s^\nu$ fits of the weak shear regime with $\nu = 0.501$ for flux and $\nu = 0.418$ for D. The blue curves correspond to γ_s^ν fits with $\nu = -1.719$ for flux and $\nu = -1.646$ for D.

TABLE I. Power-law fits for $|n(f)^2|$ scaling with shear for frequencies in 350Hz to 100kHz. Model form refers to how the shearing relates to the quantity in question, with C a constant and ν the power exponent.

Model form	γ_s regime	ν	χ^2	χ^2/ndf
$\sim 1 - C\gamma_s^\nu$	$\gamma_s \tau_{ac} < 1$	1.228	1.091	0.0642
$\sim 1 - C\gamma_s^\nu$	$\gamma_s \tau_{ac} > 1$	0.231	0.0332	0.0037
$\sim C\gamma_s^\nu$	$\gamma_s \tau_{ac} < 1$	-0.116	0.1791	0.0094
$\sim C\gamma_s^\nu$	$\gamma_s \tau_{ac} > 1$	-0.512	0.0024	0.0003

TABLE II. Power-law fits for $|v_r(f)^2|$ scaling with shear for frequencies in 350Hz to 100kHz. Model form refers to how the shearing relates to the quantity in question, with C a constant and ν the power exponent.

Model form	γ_s regime	ν	χ^2	χ^2/ndf
$\sim C\gamma_s^\nu$	$\gamma_s \tau_{ac} < 1$	0.016	0.2121	0.0117
$\sim C\gamma_s^\nu$	$\gamma_s \tau_{ac} > 1$	-0.866	0.0037	0.0005

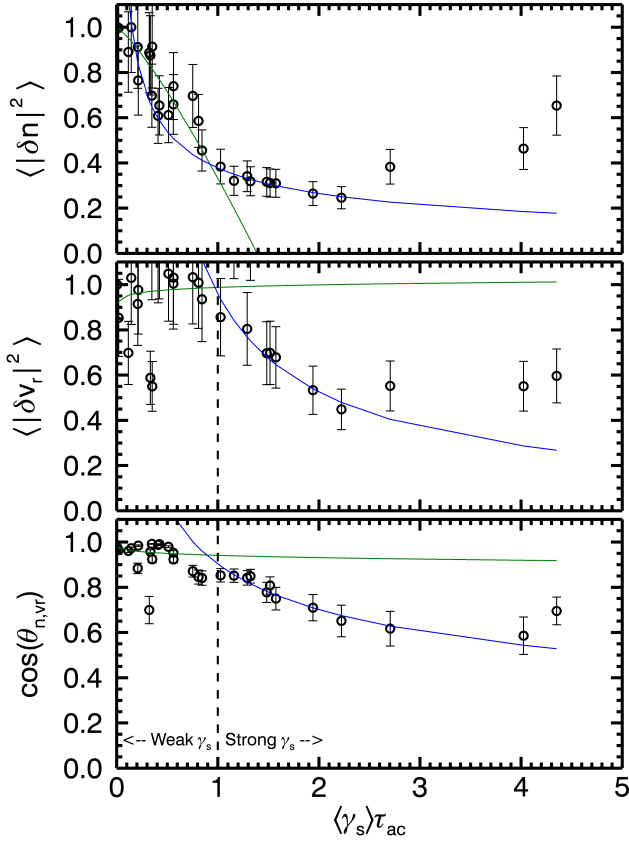


FIG. 3. Scaling of (a) density fluctuation amplitude, (b) radial velocity fluctuation amplitude, and (c) relative crossphase between density and radial velocity fluctuations. Density and velocity fluctuation are each normalized to the value at minimum shear. The green curves correspond to $1 - \gamma_s^\nu$ fits of the weak shear regime with $\nu = 0.501$ for flux and $\nu = 0.418$ for D. The blue curves correspond to γ_s^ν fits with $\nu = -1.719$ for flux and $\nu = -1.646$ for D.

TABLE III. Power-law fits for Γ_p scaling with shear for frequencies in 350Hz to 100kHz. Model form refers to how the shearing relates to the quantity in question, with C a constant and ν the power exponent.

Model form	γ_s regime	ν	χ^2	χ^2/ndf
$\sim 1 - C\gamma_s^\nu$	$\gamma_s \tau_{ac} < 1$	0.501	0.332	0.0189
$\sim 1 - C\gamma_s^\nu$	$\gamma_s \tau_{ac} > 1$	0.638	0.923	0.1110
$\sim C\gamma_s^\nu$	$\gamma_s \tau_{ac} < 1$	-0.111	0.146	0.0077
$\sim C\gamma_s^\nu$	$\gamma_s \tau_{ac} > 1$	-1.719	62.49	5.2000

TABLE IV. Power-law fits for $\cos(\theta_{nvr})$ scaling with shear for frequencies in 350Hz to 100kHz. Model form refers to how the shearing relates to the quantity in question, with C a constant and ν the power exponent.

Model form	γ_s regime	ν	χ^2	χ^2/ndf
$\sim 1 - C\gamma_s^\nu$	$\gamma_s \tau_{ac} < 1$	0.226	6.1140	0.3320
$\sim 1 - C\gamma_s^\nu$	$\gamma_s \tau_{ac} > 1$	1.274	0.0073	0.0008
$\sim C\gamma_s^\nu$	$\gamma_s \tau_{ac} < 1$	-0.020	0.0369	0.0019
$\sim C\gamma_s^\nu$	$\gamma_s \tau_{ac} > 1$	-0.365	0.0023	0.0003

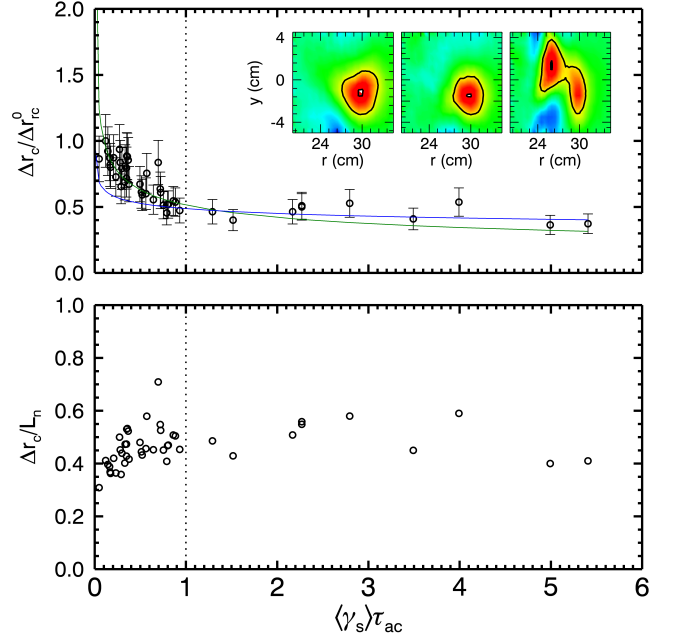


FIG. 4. (a) Radial correlation length normalized to maximum correlation length versus normalized shearing rate with correlation planes of unbiased, zero shear, and high bias states in the inset. (b) Ratio of radial correlation length to density gradient scale length.

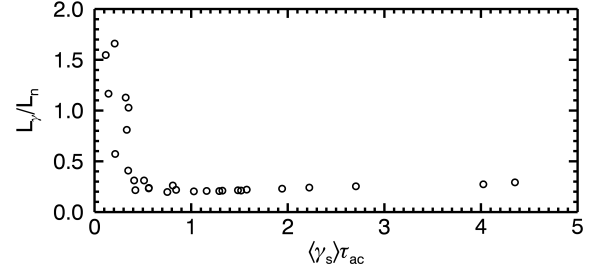


FIG. 5. Ratio of shearing length scale to density gradient length scale versus normalized shearing in the radial region of 27 to 31cm.

TABLE V. Power-law fits for $D = \Gamma_p / \nabla n$ scaling with shear for frequencies in 350Hz to 100kHz. Model form refers to how the shearing relates to the quantity in question, with C a constant and ν the power exponent.

Model form	γ_s regime	ν	χ^2	χ^2/ndf
$\sim 1 - C\gamma_s^\nu$	$\gamma_s \tau_{ac} < 1$	0.418	1.4710	0.0817
$\sim 1 - C\gamma_s^\nu$	$\gamma_s \tau_{ac} > 1$	0.197	0.0016	0.0002
$\sim C\gamma_s^\nu$	$\gamma_s \tau_{ac} < 1$	-0.217	0.4200	0.0221
$\sim C\gamma_s^\nu$	$\gamma_s \tau_{ac} > 1$	-1.646	0.0187	0.0021

TABLE VI. Power-law fits for Δr_c scaling with shear for frequencies in 350Hz to 100kHz. Model form refers to how the shearing relates to the quantity in question, with C a constant and ν the power exponent.

Model form	γ_s regime	ν	χ^2	χ^2/ndf
$\sim C\gamma_s^\nu$	$\gamma_s\tau_{ac} < 1$	-0.290	5.8730	0.1630
$\sim C\gamma_s^\nu$	$\gamma_s\tau_{ac} > 1$	-0.113	3.7040	0.3370

law in two ways reflecting in order to make comparisons to models of the form $1 - \omega^\nu$ and those of ω^ν . For the first model type, the measured quantity, y, was normalized to the value at zero shear, then transformed as $-(1 - y)$. Then, taking the logrthim of both sides, a linear fit was made for points in the weak shear and in the strong shear separately. The resulting slope of the fit is taken as the power ν . For the second type of model, no transformation of the quantity y to $-(1 - y)$ is made before the logrthms and fitting are taken. For a complete comparison to the wide range of model predictions made, fits were made for density fluctuation amplitude, radial particle flux, density-radial velocity fluctuation crossphase, radial velocity (ExB) fluctuation amplitude, radial correlation length, and experimental diffusivity ($\Gamma/\nabla n$). The best fits are summarized in Table 1 for each model type and for both weak and strong shear.

The X2/ndf is also indicated in the tables.

V. DISCUSSION

- ¹D.A. Schaffner *et al.*, Phys. Rev. Lett. **109**, 135002 (2012).
- ²K. Burrell, Phys. Plasmas **4**, 1499 (1997).
- ³P. Terry, Rev. Mod. Phys. **72**, 109 (2000).
- ⁴F. Wagner *et al.*, Phys. Rev. Lett. **49**, 1408 (1982).
- ⁵R. Taylor *et al.*, Phys. Rev. Lett. **63**, 2365 (1989).
- ⁶R. Weynants *et al.*, Nucl. Fusion **32**, 837 (1992).
- ⁷J. Boedo *et al.*, Nucl. Fusion **40**, 7 (2000).
- ⁸C. Silva *et al.*, Plas. Phys. Control Fusion **48**, 727 (2006).
- ⁹O. Sakai and Y. Yasaka and R. Itatani, Phys. Rev. Lett. **70**, 4071 (1993).
- ¹⁰J. Maggs *et al.*, Phys. Plasmas **14**, 052507 (2007).
- ¹¹T. Carter and J. Maggs, Phys. Plasmas **16**, 012304 (2009).
- ¹²K. Burrell, Phys. Plasmas **6**, 12 (1999).
- ¹³G. Tynan *et al.*, Plasma Phys. Control Fusion **51**, 113001 (2009).
- ¹⁴H. Biglari *et al.*, Phys. Fluids B. **2**, 1 (1990).
- ¹⁵E.-J. Kim *et al.*, Phys. Plasmas **11**, 10 (2004).
- ¹⁶A. Ware *et al.*, Plasma Phys. Control Fusion **38**, 1343 (1996).
- ¹⁷W.E. Amatucci *et al.*, Phys. Rev. Lett. **77**, 1978 (1996).
- ¹⁸D. Jassby, Phys. Fluids **15**, 9 (1972).
- ¹⁹W. Gekelman *et al.*, Rev. Sci. Instrum. **62**, 2875 (1991).
- ²⁰C. Holland *et al.*, Rev. Sci. Inst. **75**, 10 (2004).
- ²¹S. Zhou *et al.*, Phys. Plasmas **19**, 012116 (2012).
- ²²E. Powers, Nucl. Fusion **14**, 749 (1974).
- ²³P.W. Terry and D.E. Newman and A.S. Ware, Phys. Rev. Lett. **87**, 185001 (2001).
- ²⁴M. Umansky *et al.*, Phys. Plasmas **18**, 055709 (2011).
- ²⁵J.M. Beall and Y.C. Kim and E.J. Powers, J. Appl. Phys. **53**, 6, 1982.